Building and Environment 212 (2022) 108837

Contents lists available at ScienceDirect

Building and Environment

journal homepage: www.elsevier.com/locate/buildenv

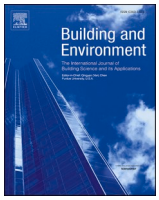

Directional characterisation of annual and temporary exposure to rainwater penetration on building façades throughout Mexico

José M. Pérez-Bella [a,*], Javier Domínguez-Hernández [a], Juan J. del Coz-Díaz [b], Juan E. Martínez-Martínez [b]

[a] Department of Construction Engineering, Engineering and Architecture School, University of Zaragoza, María de Luna, s/n, 50018, Zaragoza, Spain
[b] Department of Construction Engineering, University of Oviedo, Edificio Departamental Viesques n° 7, 33204, Gijón, Spain

ARTICLE INFO

Keywords:
Wind-driven rain
Wind pressure
Façade design
Rainwater penetration
Mexico
Tropical cyclones

ABSTRACT

Rainwater penetration on building façades has a significant impact on the durability, hygrothermal performance, and habitability of buildings. This research characterises the directional exposure of Mexican façades to rainwater penetration by identifying wind-driven rain (WDR) and driving rain wind pressure (DRWP) throughout the country. For this purpose, climatic datasets of daily resolution gathered at 527 weather stations between 2003 and 2018 were analysed. As a result, isopleth maps of annual scalar values of WDR, DRWP, and the approximate orientation of their directional maxima were produced. The joint risk of rainwater penetration (defined by both factors) and the applicability of novel extrapolation that estimates the maximum directional exposures anywhere in Mexico from scalar results are also discussed. Additionally, the influence of certain tropical cyclones on the exposure was characterised, leading to the identification of preliminary patterns associated with these temporary WDR and DRWP exposures. Such extreme climatic events can cause, in a short interval of time, as much WDR as that occurring during the rest of the year and DRWP that is 2–5 times higher than the mean annual value. In general, the highest level of hazard of rainwater penetration on façades was identified west of the Isthmus of Tehuantepec and on the coast of the state of Veracruz.

1. Introduction

Throughout its vast territory (1,964,375 km^2), Mexico presents pronounced climatic and topographical variability with large areas that are seasonally subjected to extreme precipitation and wind (e.g. tropical cyclones) [1,2]. Despite this, the country lacks characterisation of rainwater penetration risk for its façades; consequently, applicable building codes and design standards have significant improvement potential [3].

It is well known that water ingress into façades has a significant impact on the energy consumption of buildings, reduces the durability of construction materials, and affects the health of inhabitants [4–9]. This penetration occurs when rainwater runoff overcomes the pressure thresholds of surface tension and capillary pressure of the water contained in the porous construction materials [10,11]. For this, a combination of two atmospheric phenomena is necessary: rainwater supply impacting the façade surface (wind-driven rain or WDR) and the simultaneous action of the wind pressure on surface water runoff (driving rain wind pressure or DRWP) [11–14].

For the first time in Mexico, the scalar and directional values of WDR and DRWP were determined by semi-empirical methods to characterise the exposure distribution throughout the territory, analysing available daily datasets of rainfall and wind velocity gathered in 527 automatic weather stations from 2003 to 2018. Moreover, both phenomena were combined into a single index to determine the comparative risk of water penetration by the location [14,15]. Based on the isopleth maps produced from the WDR and DRWP scalar results, further extrapolation could functionally estimate the maximum directional values at any site of the territory [16].

Finally, some notable tropical cyclones that occurred during the studied interval were selected. Their specific contribution to the annual values of WDR and DRWP was analysed at locations that were on their path. Thus, preliminary patterns concerning the temporary exposures caused by this type of extreme climatic events were identified.

Such a comprehensive analysis will enable to replace the current generic design requirements for Mexican façades with performance-

* Corresponding author. Department of Construction Engineering, University of Zaragoza (UZ), María de Luna, s/n, 50018, Zaragoza, Spain.
E-mail address: jmpb@unizar.es (J.M. Pérez-Bella).

https://doi.org/10.1016/j.buildenv.2022.108837
Received 17 November 2021; Received in revised form 21 January 2022; Accepted 23 January 2022
Available online 1 February 2022

based requirements throughout the country. In addition, the characterisation of the Mexican territory is particularly interesting given the high altitude of many populated areas (e.g. Mexico City is located at more than 2,000 m above sea level) and the recurrence of extreme climatic events [1,2,17].

2. Background

The characterisation of WDR and DRWP can be mainly performed with *(i)* experimental measurements, *(ii)* applying numerical methods based on computational fluid dynamics, and *(iii)* by means of semi-empirical approaches [18,19]. The first two procedures can be resource-intensive (in terms of time, instrumentation, or calculation effort) and are mostly applicable to specific local contexts [20,21]. In turn, semi-empirical approaches use climatic records available from weather stations, allowing a functional characterisation in large areas and under assorted weather conditions (although less accurate than the prior methods). Therefore, many semi-empirical studies have recently been developed as a preliminary step to define improved design requirements for façade watertightness in different regions [14,15,22–27].

The semi-empirical approaches for calculating wind-driven rain are based on the overall 'WDR relationship' proposed by Lacy and Shellard [28], which allows estimating the rainfall deflected by the wind that passes through a vertical plane in free-field conditions. This relationship can be obtained by multiplying simultaneous records of rainfall intensity R_h (l/m^2) and wind speed U (m/s), and it is adjusted by a variable empirical coefficient k (s/m), which is inversely related to the terminal falling speed of raindrops (Eq. (1)) [29]. Then, the directional value of wind-driven rain WDR_θ (l/m^2) can be determined by adding a cosine projection that considers the simultaneous record of wind direction D (°) and the orientation of the analysed façade θ (°).

$$WDR_\theta = k \cdot U \cdot R_h \cdot \cos(D-\theta) \tag{1}$$

For decades, the most widespread application of the WDR relationship has been the so-called Driving Rain Index (DRI), because *(i)* it ignores the indeterminacy caused by the empirical coefficient k, which can vary between 0.1 and 0.5 s/m according to climatic conditions, and *(ii)* it allows the use of varied climatic records unlike more accurate approaches, such as the one stablished by standard ISO 15927–3 (requiring long series of hourly records, which are unavailable in many regions) [28–30]. This index (Eq. (2)) offers a representative characterisation of the annual WDR ($aDRI_\theta$) (m^2/s) that is comparable between different locations and can be calculated from the climatic records commonly gathered at any site over N years. In the summation are only considered the m recording intervals in which the wind direction D (°) affects the analysed façade orientation θ (°) (i.e. cosine projections with positive values). Despite the frequent use of monthly and annual records to produce regional exposure maps (*maDRI* and *aaDRI*, respectively), a recent study has shown the significance of using at least daily records to ensure adequate accuracy (i.e. $daDRI_\theta$) [31].

$$daDRI_\theta = \frac{\sum_{i=1}^{m} U_i \cdot \left(\frac{R_{h,i}}{1000}\right) \cdot \cos(D_i-\theta)}{N} \tag{2}$$

This functional index could also be adjusted by considering generic coefficients k as well as 'wall indices' that represent the topography and surroundings of each specific façade, in a similar way the standard ISO 15927-3 suggests. All these characteristics, in addition to the possibility of omitting the cosine factor to obtain scalar results, explain the widespread acceptance of this index in WDR studies [14,15,18,22–27].

Furthermore, the characterisation of the $DRWP_\theta$ exposure (Pa) is generally based on Bernoulli's equation (Eq. (3)), where ρ_{air} represents the air density (normally 1.2 kg/m^3) and C_p (−) is the pressure coefficient (usually set at 1). The summation only considers the available p wind speed records U (m/s) gathered during the analysed period that are simultaneous to precipitation ($p \leq m$; see Eqs. (2) and (3)) and also impact the façade orientation analysed (again, only cosine projections with positive values). These distinctive features prevent the direct use of mean wind pressure values as DRWP, making necessary a specific analysis of simultaneous climatic records for every possible façade orientation.

$$dDRWP_\theta = \frac{\sum_{i=1}^{p} C_p \cdot \frac{1}{2} \cdot \rho_{air\ i} \cdot U_i^2 \cdot \cos(D_i-\theta)}{k} \tag{3}$$

Records of different resolutions can also be used (e.g. monthly and yearly); however, for the DRWP, even daily data can cause non-negligible errors (i.e. in $dDRWP_\theta$) [31]. In this way, the accuracy of this directional characterisation is limited by the daily climatic records available in each region.

Although studies of DRWP have not received as much attention as those of WDR, its key importance for rainwater penetration processes is recognised by all standardised watertightness tests for building façades [12,32]. In general, the smaller the size of pores, defects, and cracks on the façade surface, the more relevant the DRWP is to promote water progression [10,33]. Consequently, its study receives increasing attention [10,13–15,34].

In any case, neither of the indices can completely characterise the risk of rainwater penetration into building façades; this penetration can be produced by the combination of both high WDR - low DRWP values and low WDR - high DRWP values, depending on the characteristics of the construction materials. In addition, the aDRI and DRWP indices cannot be directly added or averaged, as they do not represent comparable physical magnitudes.

To characterise the joint risk represented by these factors, a functional approach is achieved by using the risk index of water penetration (RIWP), which combines normalised values of these indices in the set of analysed locations [14,15,26]. Scalar exposures are used to calculate the normalised values (removing the cosine projection component of Eqs. (2) and (3)), allowing a single risk characterisation by the location. Hence, this index generically represents the joint severity of the climatic conditions at each site, making it possible to compare the overall risk of rainwater penetration of each studied location regarding the other sites included in the sample (Eq. (4)).

$$RIWP_j = \sqrt{\alpha \cdot \left(aDRI_{normalised\ j}\right)^2 + \beta \cdot \left(DRWP_{normalised\ j}\right)^2} \tag{4}$$

The normalised indices $aDRI_{normalised}$ and $DRWP_{normalised}$ adopt a value between 0 and 1, depending on the scalar exposure of each site j in relation to the maximum and minimum values within the studied region (Eqs. (5) and (6)). As a result, the *RIWP* (−) is higher at locations with increased combined exposures, ranging from 0 to $\sqrt{2}$.

$$aDRI_{normalised\ j} = \frac{aDRI_j - aDRI_{\min}}{aDRI_{\max} - aDRI_{\min}} \tag{5}$$

$$DRWP_{normalised\ j} = \frac{DRWP_j - DRWP_{\min}}{DRWP_{\max} - DRWP_{\min}} \tag{6}$$

The weighting coefficients α and β may be used to represent the relative influence of WDR and DRWP in the penetration process, thereby adjusting the RIWP results for different purposes (e.g. heritage policies and normative actions for new buildings). For a non-specific purpose, as the one addressed in this work (i.e. deteriorated and new building façades with variable pore sizes, cracks, and defects in the surface finishes), a value equal to 1 for α and β can be adopted considering an equal influence of both factors on rainwater penetration. This characterisation could be refined in the future by defining proper weights for different situations.

A directional analysis of WDR and DRWP for 527 weather stations in Mexico is presented in Section 3. For this, daily record series associated with periods of 5–12 years of duration were considered. There is noticeable variation of characterisation between Mexican states, both in

number of weather stations and in years of available data; therefore, to the authors' knowledge, the obtained results (i.e. *daDRI*, $daDRI_\theta$, *dDRWP*, and $DRWP_\theta$) represent the most ambitious study addressed so far in Mexico in this regard. The resulting isopleth maps provide, for the first time, a view of the exposure to rainwater penetration into building façades throughout the country.

In Section 4 is exposed a combination of those maps with a recent approach that functionally estimates the most unfavourable directional value from scalar values. This allows directional characterisation throughout the country (not only at the 527 sites analysed here) [19]. The overall risk of rainwater penetration by combining the WDR and DRWP exposures (i.e. *RIWP*) is also analysed. Finally, the temporary WDR and DRWP values caused by extreme climatic events (i.e. some representative tropical cyclones) were also analysed, providing preliminary patterns that can complement the annual characterisation to be considered for the façade design against rainwater.

3. Characterisation of directional WDR and DRWP values in Mexico

In this study, the exposure to rainwater penetration in Mexican façades was assessed from simultaneous daily datasets of rainfall intensity and wind velocity (speed and direction) that were provided by official Mexican organisations for the interval between 2003 and 2018 [35,36]. The analysis of weather stations having less than 5 years of available data has been discarded. In addition, the analysed period (greater than or equal to 5 years) must present less than 15% of missing data, for which those complete years that prevent reaching this threshold have been also discarded. The mean value of suitable data in the selected stations reached 94.7% (see Table 1 and the supplementary material).

A result of this screening protocol, which intends to ensure certain representativeness of the results obtained, is that the characterisation of the country has been heterogeneous. The centre of Mexico, which is highly populated and therefore of great interest for the assessment of façade exposure conditions, has been exhaustively characterised. In contrast, the peninsulas of Baja California and Yucatán as well as the states of Nayarit, Jalisco, Michoacán, and Guerrero have considerably fewer weather stations that reach the acceptance thresholds. The selected and analysed weather stations (527 in total, 1 site per 3,727 km^2 on average, which would be equivalent to one station in the centre of a 61 × 61 km square) were located near population centres and agricultural holdings, complying with the requirements established by the World Meteorological Organization for the recording of climatic data (adequate elevation of the anemometer and location in open field) [37].

The altitudes of the selected locations ranged from 1 m (Pozo Peña station, Baja California Sur) to 2,733 m (El Vergel station, Chihuahua) with an average of 1,074 m above sea level. These high altitudes are typical of the Mexican territory, characterised by large mountain ranges that cover most of the country (Fig. 1). The Sierra Madre Occidental (along the coast of the Gulf of California) and the Sierra Madre Oriental (along the coast of the Gulf of Mexico) stand out for their range. Between them is located an extensive plateau with increasing altitude from the northern border of Mexico (around 800 m) to the south, extending to the Trans-Mexican Volcanic Belt. This volcanic mountain range crosses the centre of the country from coast to coast, including the highest elevations of Mexico (Pico de Orizaba, 5,610 m; Popocatépetl, 5,500 m) as well as the largest urban concentrations (almost 22 million people live only in Greater Mexico City, ignoring irregular settlements). Smaller mountain ranges, such as the Sierra Madre del Sur (Guerrero and Oaxaca states, reaching 3,710 m) and the Sierra Madre de Chiapas (Tacaná volcano, 4,080 m) are found farther southeast and are separated by the Isthmus of Tehuantepec. Only in the broad coastal plains of the Gulf of Mexico (Tamaulipas, Veracruz, and the Yucatán Peninsula) and on the coast around the Gulf of California, the altitude is lower than 1,000 m.

Table 1
General overview of the analysed weather stations.

Years of available data	Number of stations	Avg. altitude (m)	Avg. missing data (%)
5	137	453	5.85
6	86	1,160	6.06
7	87	881	6.63
8	56	1,067	6.27
9	48	1,381	4.46
10	88	1,889	2.26
11	23	1,431	5.29
12	2	1,122	4.46
Mexican stations	**527**	**1,074**	**5.30**

This mountainous topography, mainly volcanic, has a great influence on the climate, reducing rainfall far from the coast and modifying the prevailing winds in each region (also the directional values of WDR and DRWP). The climate of the country is characterised by its great variety, and three large zones can be distinguished (Fig. 1): the north, characterised by deserts, steppes, and Mediterranean climates; the Atlantic and Pacific coast south of the Tropic of Cancer, with tropical climates; and the centre of the country (Trans-Mexican Volcanic Belt and Sierra Madre del Sur) characterised by humid, subtropical, and oceanic climates.

In general, the mean annual rainfall matches this climatic distribution, presenting values in northern Mexico that range from less than 100 $l/m^2{\cdot}yr$ (Baja California Peninsula) to almost 600 $l/m^2{\cdot}yr$ (mountainous areas of the Sierra Madre Occidental and Sierra Madre Oriental) and progressively increases toward the coasts and southeast of the country, reaching up to 4,000 $l/m^2{\cdot}yr$ around the Isthmus of Tehuantepec (states of Veracruz, Oaxaca, Tabasco, and Chiapas) [1]. In turn, the highest wind speeds were identified in exposed coastal areas (Michoacán, Tamaulipas, Veracruz, and southern Baja California Peninsula) as well as in the plains of the Yucatán Peninsula and in the centre of the country (in this case due to the higher altitude).

In addition, broad regions of Mexico are subject to the seasonal passage of extreme atmospheric events such as tropical cyclones. These occur when large masses of warm and humid air develop around areas of low pressure over the Atlantic and Pacific oceans, favoured by the high water temperature (Caribbean and North Equatorial warm currents) and by rotating winds around latitudes 5°-15° N. Their peak of activity occurs between August and September, with paths from east to west (due to the action of the trade winds), which lead them to impact on both coasts of the country [2,39].

These tropical cyclones significantly increase the annual value of WDR and DRWP and define the maximum temporary exposure that the Mexican building façades must resist [40]. Some of the most hazardous events within the studied period (according to the Saffir-Simpson scale) were considered for further analysis as explained in Section 4.2: Dean (August 2007), Alex (June 2010), Karl (September 2010), and Odile (September 2014) [41,42].

3.1. WDR and DRWP results

The scalar *daDRI* and *dDRWP* values in the 527 locations (i.e. mean annual values) were calculated using Eqs. (2) and (3) by eliminating the cosine term from the formulation. In addition, a directional analysis was performed by discretising the possible façade orientations θ at 15° intervals. As a result, 24 directional values of mean annual exposure were obtained at each weather station (i.e. $daDRI_\theta$ and $dDRWP_\theta$ values). Tables 2 and 3 show the sites characterised by higher scalar values, also presenting the maximum directional value of each location and the orientation of the façade on which it occurs. For clarity, the full list of results by the location is provided in the supplementary material of this paper.

To facilitate the analysis of these results, the scalar values obtained at the 527 locations were linearly interpolated on the basis of a triangle mesh, thus producing smoothed isopleths of exposure. The resulting

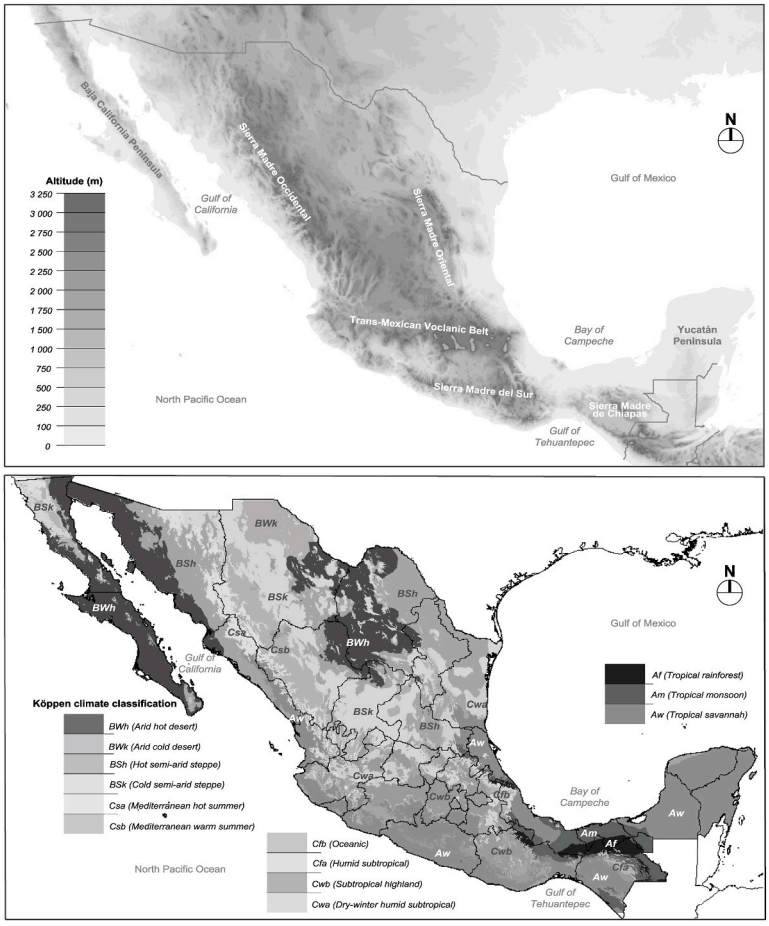

Fig. 1. Top: Hypsometric map of Mexico, Bottom: Köppen-Geiger climate classification map [38].

Table 2
Weather stations with the highest WDR values (scalar *daDRI* higher than 5 m^2/s).

Weather staton (state)	Latitude (DD)	Longitude (DD)	Altitude (m)	Data range and missing data (%)	*daDRI* (m^2/s)	*Max. daDRI*$_\theta$ (m^2/s)	*Orientation of max.* (°)
La Mina (Oaxaca)	−96.109	17.978	20	2008/14 (9.82)	22.52	15.48	300
La Posta (Veracruz)	−96.329	19.319	7	2008/15 (6.95)	14.20	10.55	0
Amatitlan (Veracruz)	−95.713	18.485	612	2009/16 (13.53)	12.34	6.47	255
Cerro Chango (Oaxaca)	−96.285	18.175	35	2008/13 (6.79)	8.05	5.27	270
La Granja (Veracruz)	−96.241	18.382	40	2010/16 (10.46)	7.80	7.31	15
El Porvenir (Oaxaca)	−95.314	17.451	111	2008/14 (10.10)	7.04	6.42	315
S. Nicolás (Veracruz)	−96.901	18.790	300	2008/15 (5.71)	6.86	3.99	300
El Progreso (Oaxaca)	−95.549	17.526	440	2008/14 (10.23)	6.61	5.17	270
Loma Bonita (Oaxaca)	−95.849	17.981	72	2008/14 (5.68)	6.36	5.97	315
Úrsula Gaván (Veracruz)	−96.358	19.414	13	2007/14 (9.67)	5.87	4.14	345
Ignacio Palotal (Veracruz)	−96.272	18.942	29	2008/15 (7.01)	5.66	3.58	15
Mundo Nuevo (Oaxaca)	−96.145	18.121	20	2008/15 (7.40)	5.41	3.58	270
El Tomatal (Oaxaca)	−96.940	15.797	48	2012/16 (10.25)	5.14	3.35	15
La Tee (Quintana Roo)	−88.527	18.534	31	2009/13 (4.65)	5.00	4.16	45

Angles are measured in degrees from the north.

maps allow the identification of scalar *daDRI* and *dDRWP* values anywhere in Mexico as well as the analysis of their geographical distribution throughout the territory (see Figs. 2 and 3).

By analysing the mean annual WDR values, the most exposed areas were identified in the states of Veracruz and Oaxaca, especially in the plain between the Trans-Mexican Volcanic Belt, the Sierra Madre del Sur, and the Isthmus of Tehuantepec (see Table 2 and Fig. 2 -at the top-). This area combines strong coastal winds and high rainfall, which diverts a large amount of rainwater to the vertical surface of the building façades. Moderate values were identified in specific zones of the main mountain ranges of the country as well as in the highest areas of the Yucatán Peninsula. However, most of the country is characterised by *daDRI* values that are usually less than 2 m^2/s. The relationship between rainfall and WDR is not reliable, since, for example, the states of Chiapas and Tabasco do not present considerable WDR values. This fact highlights the need for conducting specific WDR studies (like the one presented here) and rejecting design requirements based on generic climatic and rainfall maps [3].

Fig. 2 (bottom) represents the orientation of the façades most exposed to the WDR throughout the territory. The map was obtained by

Table 3
Weather stations with the highest DRWP values (scalar *dDRWP* higher than 30 Pa).

Weather staton (state)	Latitude (DD)	Longitude (DD)	Altitude (m)	Data range and missing data (%)	*dDRWP* (Pa)	*Max. dDRWP*$_\theta$ (Pa)	*Orientation of max.* (°)
La Granja (Veracruz)	−96.241	18.382	40	2010/16 (10.46)	181.63	211.78	30
Álamo (Veracruz)	−97.680	20.934	53	2008/13 (14.30)	167.39	219.47	0/360
La Posta (Veracruz)	−96.329	19.319	7	2008/15 (6.95)	122.40	147.18	195
La Conquista (Veracruz)	−96.379	19.293	58	2008/14 (7.45)	67.97	62.61	180
El Tomatal (Oaxaca)	−96.940	15.797	48	2012/16 (10.25)	52.14	42.83	45
Tlacolula (Veracruz)	−97.948	21.091	520	2009/14 (14.83)	47.84	59.31	15
La Mina (Oaxaca)	−96.109	17.978	20	2008/14 (9.82)	45.56	40.51	15
Tepeaca (Puebla)	−97.901	18.989	2235	2006/13 (6.18)	43.58	39.05	90
Tabacalera Turrent (Veracruz)	−95.134	18.429	420	2007/15 (8.55)	41.36	41.36	255
Úrsula Gaván (Veracruz)	−96.358	19.414	13	2007/14 (9.67)	39.12	34.66	180
Amatitlan (Veracruz)	−95.713	18.485	612	2009/16 (13.53)	34.46	40.24	195
Rodríguez Clara (Veracruz)	−95.329	17.995	97	2007/15 (7.90)	34.19	35.85	330
Rancho Alfonso (Puebla)	−97.403	19.308	2373	2006/11 (4.98)	32.70	26.13	330

Angles are measured in degrees from the north.

interpolating linearly the orientation of maximum exposure identified in the 527 stations within a triangle mesh, discretised, for clarity, in only four orientations: northeast (0-90° from the north), southeast (90-180°), southwest (190-270°), and northwest (270-360°). As can be observed, there is greater variability in mountainous areas due to the complex topography and its interaction with the prevailing winds during precipitation events. In a quite simplified way, it is possible to distinguish maximum exposures of the east of the country (with maximum values predominantly coming from the northwest and northeast) from those in the west (where maximum exposures coming from the southeast and southwest are common).

The areas characterised by high DRWP values are located in the states of Veracruz (south of the Tamiahua Lagoon), Puebla, and Oaxaca (southern part of this state), especially near the coasts (Table 3 and Fig. 3 [top]). These results are consistent with the persistence of strong coastal winds and with the frequent impact of tropical cyclones. Other areas, such as the surroundings of the Cumbres de Majalca National Park (Chihuahua), also presented notable DRWP values. However, most of the country presents wind speed values (simultaneous to the precipitation) that are not prominent, with annual mean DRWP values lower than 5 Pa.

As can be observed in Fig. 3 (bottom), the orientation of the most exposed façades to DRWP varies notably throughout the country, especially in the mountain ranges. In general, on the Pacific coast, the maximum exposures predominate on northeast- and southeast-facing façades, whereas on the Atlantic coast, façades facing northwest and northeast tend to be the most exposed. Specifically, northwest-facing façades in the north coast of the Isthmus of Tehuantepec, northern Tamaulipas, and the most exposed coastal areas of the Yucatán and Baja California peninsulas present maximum exposures.

4. Discussion

A recent study, in which Mexican climatic data have also been considered, showed that it is possible to estimate with reasonable accuracy the maximum directional values of WDR and DRWP from the scalar values associated with each location [16]. Both *daDRI* and *dDRWP* scalar values can be obtained without significant calculation efforts even at sites without wind direction records; this enables a simpler and more accessible characterisation of maximum directional exposure for the entire country.

Owing to functional and economic considerations, it is common for all façade orientations of a building to incorporate a common constructive solution. Usually, only the thickness of the thermal insulation and the size/disposition of the openings vary according to the façade orientation [43]. This means that only the directional exposure value of the most unfavourable orientation is relevant for the design of façades against rainwater penetration (regardless of what this orientation is).

Fig. 4 shows the best-fit relationships between the scalar and maximum directional values for both the WDR and DRWP (black lines). The high coefficients of determination R^2 reveal a strong correlation between these magnitudes despite the wide variety of climates, altitudes, and geographic surroundings represented by the 527 weather stations [44]. Given that this study incorporates a greater number of Mexican locations (also rejecting weather stations with less than five years of data), both best-fit relationships are slightly more accurate and representative than those identified in the previously mentioned study [16]. These relationships are also similar to those identified in Spain, Norway, and Chile (dotted lines) [16,26] and can be refined to obtain more specific relationships (e.g. by Mexican state) by considering only the weather stations of each state (see the supplementary material). For both WDR and DRWP, the errors remained below 20% in most locations (shaded zones in Fig. 4). Large percentage errors can be identified in some stations with moderate and low exposure, although the quantitative error also becomes less significant as the exposure value decreases.

The goodness-of-fit ($R^2 = 0.94$ for WDR and 0.98 for DRWP) guarantees the accuracy of these general formulae for estimating, in a functional way, the most unfavourable directional exposure from the scalar maps presented in Figs. 2 and 3. In addition, when combining this estimation with the orientation maps (at the bottom of both figures), it is possible to identify unfavourable façade orientations anywhere in the country. Together, these results provide a simple, reliable, and comprehensive tool for the design of Mexican building façades against rainwater penetration.

4.1. Combined exposure and rainwater penetration

The RIWP calculated with Eqs. (4)–(6) allows characterising the joint contribution of both the WDR and DRWP to rainwater penetration as well as comparing this combined exposure for the different sites. Table 4 shows the Mexican weather stations subjected to the most unfavourable combined conditions, generically considering α and β values equal to 1 (see Eq. (4)).

As can be seen, the façades under the highest joint exposure are located in the states of Veracruz and Oaxaca, suggesting their need to establish more demanding watertightness design requirements. It is worth noting how the two most exposed locations present very different characteristics: In La Granja (Veracruz), the most determining factor is the high wind speed simultaneous to precipitation, whereas in La Mina (Oaxaca), it is the high rainwater supply on the façades.

The partial contribution of each factor can be seen in Fig. 5 (bottom), where the RIWP value corresponds to the distance from the site (points) to the origin and the greatest influence of one or the other factor, to its

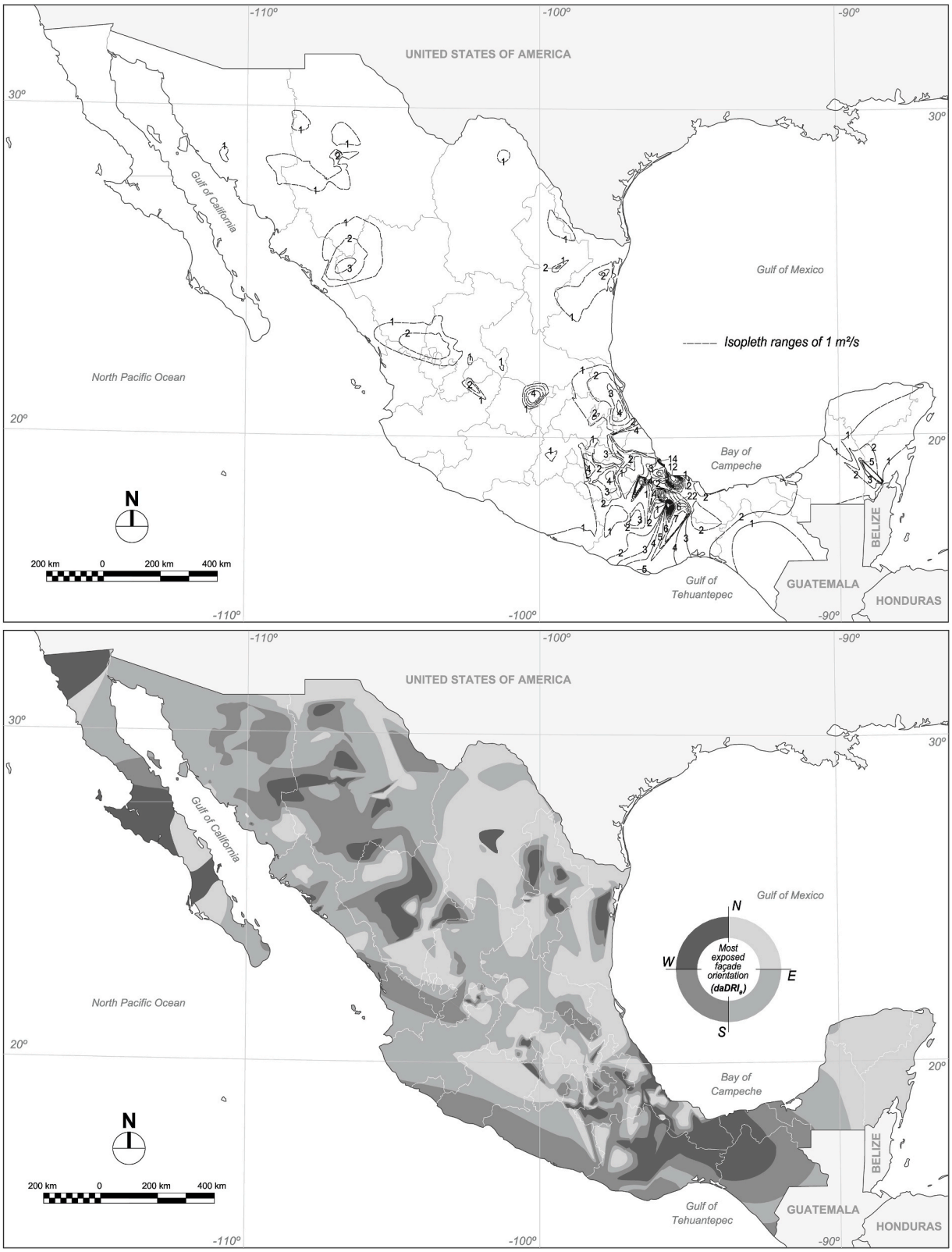

Fig. 2. Top*: daDRI* isopleth map of Mexico (from daily records gathered between 2003 and 2018), Bottom: Orientation of the most exposed façades.

position with respect to the bisector. Although a limited number of locations present a comparatively high risk, most of the points are concentrated near the origin (i.e. low RIWP values). Only six of the 527 stations (1.14%) had RIWP values higher than 0.4. This is a much lower value than that identified in countries, such as Brazil (41%), Chile (45%), and Spain (15%) [14,26,45]. These demonstrate a clear distinction between a minority of sites that are subjected to a great relative risk of rainwater penetration (especially in the states of Veracruz and Oaxaca) and a vast majority of locations that are subjected to very low exposures (just comparing the exposures relative to the 527

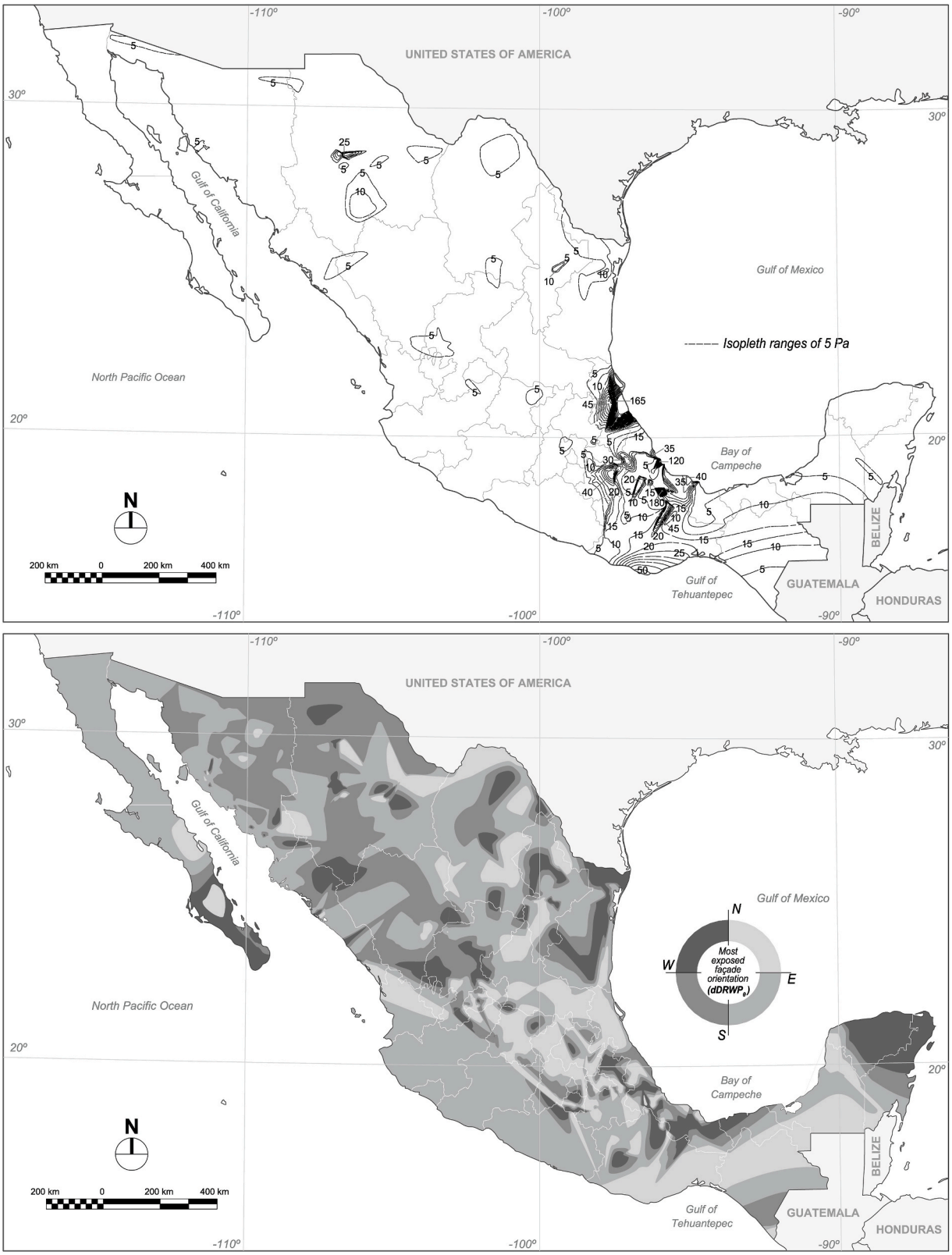

Fig. 3. Top: *dDRWP* isopleth map of Mexico (from daily records gathered between 2003 and 2018), Bottom: Orientation of the most exposed façades.

stations analysed throughout the country).

In addition, in most locations, the main risk factor corresponds to the high rainwater supply on the façades (points shown below the bisector in Fig. 5). Consequently, deteriorated or insufficiently maintained buildings are the most vulnerable to this penetration (the existence of openings and cracks larger than 5 mm allows the ingress of rainwater even without significant DRWP values) [10]. Only in some areas (especially in Veracruz), new buildings or those with surface deficiencies of less than 1 mm could present rainwater penetration problems caused by high wind pressures concurrent with precipitation

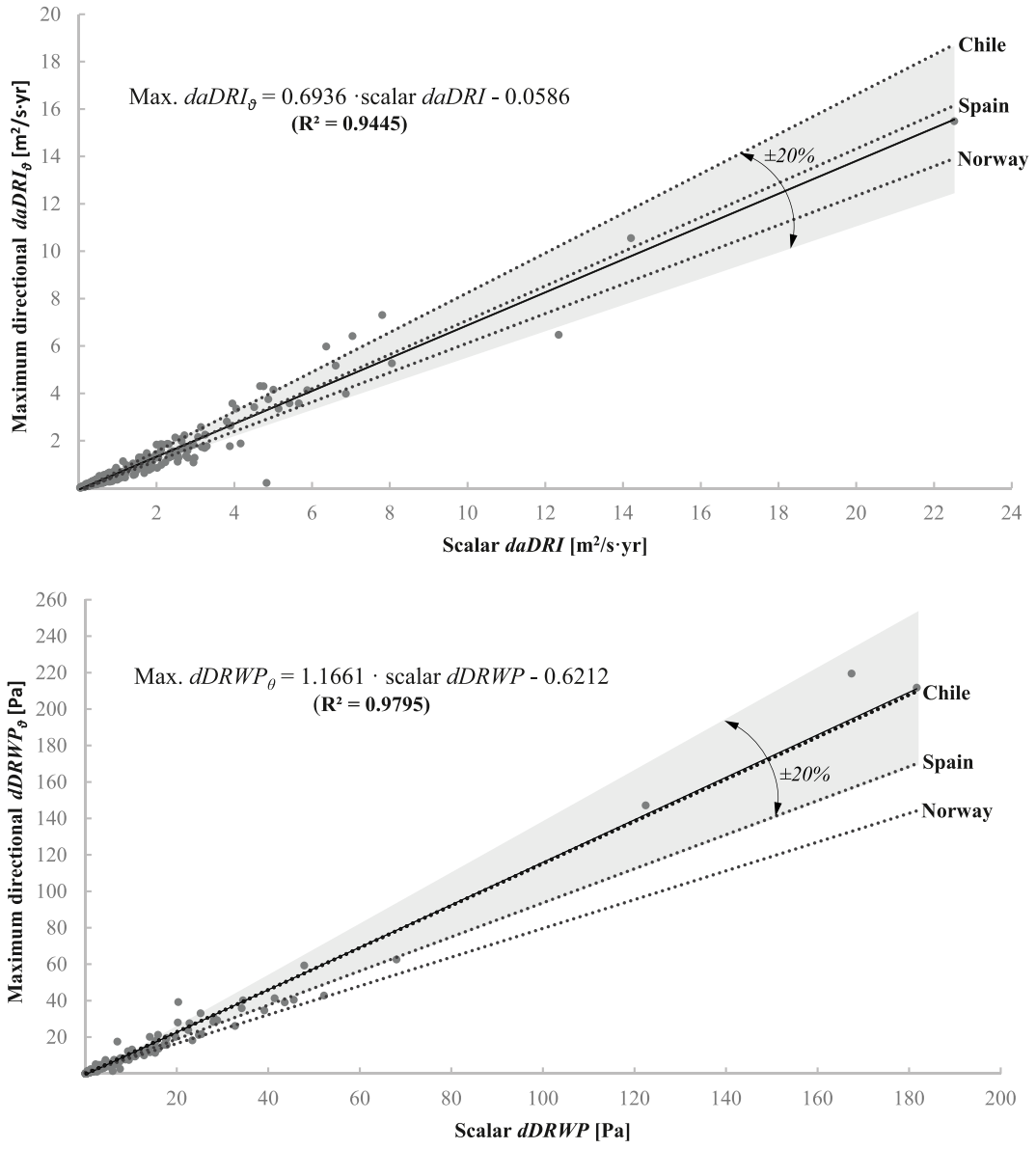

Fig. 4. Best-fit relationship between scalar and maximum directional values for the analysed locations.

Table 4
Weather stations with a *RIWP* value higher than 0.3.

Weather staton (state)	Latitude (DD)	Longitude (DD)	Altitude (m)	Data range and missing data (%)	*daDRI* (m^2/s)	*dDRWP* (Pa)	*RIWP value* (–)
La Granja (Veracruz)	−96.241	18.382	40	2010/16 (10.46)	7.80	181.63	1.06
La Mina (Oaxaca)	−96.109	17.978	20	2008/14 (9.82)	22.52	45.56	1.03
Álamo (Veracruz)	−97.680	20.934	53	2008/13 (14.30)	4.04	167.39	0.94
La Posta (Veracruz)	−96.329	19.319	7	2008/15 (6.95)	14.20	122.40	0.92
Amatitlan (Veracruz)	−95.713	18.485	612	2009/16 (13.53)	12.34	34.46	0.58
La Conquista (Veracruz)	−96.379	19.293	58	2008/14 (7.45)	3.80	67.97	0.41
El Tomatal (Oaxaca)	−96.940	15.797	48	2012/16 (10.25)	5.14	52.14	0.37
Cerro Chango (Oaxaca)	−96.285	18.175	35	2008/13 (6.79)	8.05	10.23	0.36
Úrsula Gaván (Veracruz)	−96.358	19.414	13	2007/14 (9.67)	5.87	39.12	0.34
S. Nicolás (Veracruz)	−96.901	18.790	300	2008/15 (5.71)	6.86	22.76	0.33
Loma Bonita (Oaxaca)	−95.849	17.981	72	2008/14 (5.68)	6.36	27.97	0.32
El Porvenir (Oaxaca)	−95.314	17.451	111	2008/14 (10.10)	7.04	13.89	0.32
Tepeaca (Puebla)	−97.901	18.989	2235	2006/13 (6.18)	4.16	43.58	0.30

events.

This analysis of this joint exposure was complemented by the graphic representation of its territorial distribution as shown in Fig. 5 (top). As expected, most regions have combined WDR-DRWP values that are much lower than those of northern Sierra Madre del Sur. Thus, the greatest risk was identified in the plains of the state of Veracruz, the northern foothills of the aforementioned Sierra (within the state of Oaxaca), and in the easternmost zone of the Trans-Mexican Volcanic

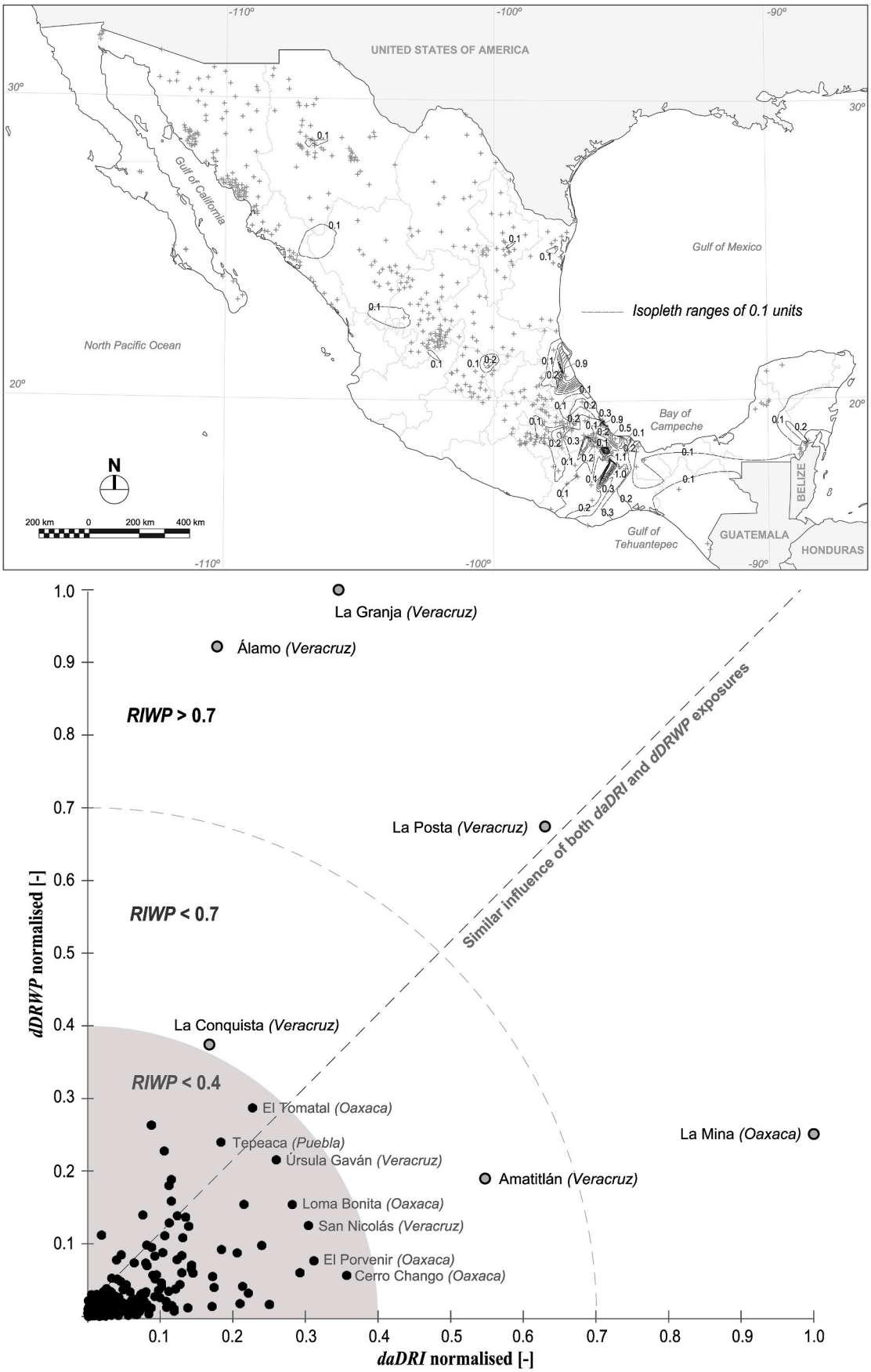

Fig. 5. Top: *RIWP* isopleth map of Mexico *(the 527 sites analysed are shown by crosses)*, Bottom: *RIWP* scheme for the analysed locations.

Belt.

4.2. Temporary exposures caused by tropical cyclones

Although rainwater penetration on façades occurs throughout the year, this process intensifies during specific intervals of sustained and high exposure to WDR and DRWP. During these wetting intervals, normally associated with the passage of low-pressure areas, the water supply can greatly exceed the evaporation loss causing a temporary exposure that is not represented by the mean annual values [25,30,46].

The most unfavourable wetting intervals that the Mexican building façades must withstand occur during the seasonal passage of tropical cyclones. The high rainfall and wind speeds associated with these atmospheric events (sometimes catastrophic in nature) cause temporary WDR and DRWP exposures of great intensity [47,48]. As a first approximation, this study identified the temporary WDR and DRWP values in some of the stations located in the path of four tropical cyclones occurring within the range of available climate data (see Fig. 6). These cyclones encompass impacts on different latitudes and coasts of the country and are classified among the most intense according to the

Tropical cyclone ***Dean*** (Atlantic Ocean)
Category 5. First impact on land: August 21, 2007
Affected zones: Campeche, Hidalgo, Puebla, Querétaro, Quintana Roo and Veracruz

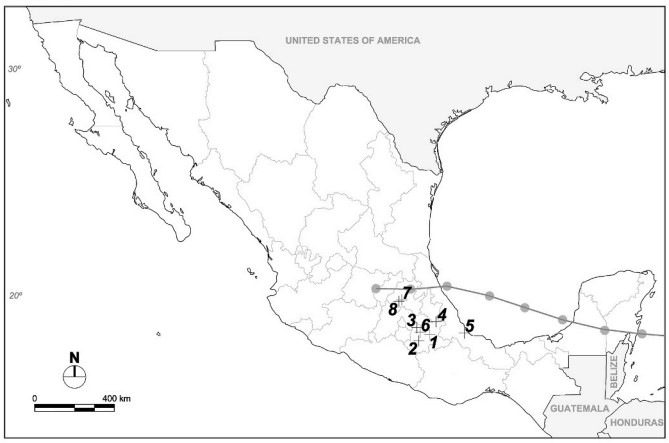

No.	Weather stations	2007 *daDRI* [m²/s]	Event contribution [m²/s]	2007 *dDRWP* [Pa]	Peak of the event [Pa]
1	Tepeaca (Puebla)	9.107	2.603 (28.6%)	70.448	162.559 (x2.31)
2	Los Monjes (Puebla)	5.109	3.122 (61.1%)	18.153	29.991 (x1.65)
3	S. Miguel Contla (Puebla)	4.410	1.168 (26.5%)	12.089	25.820 (x2.14)
4	Payuca (Puebla)	3.708	2.082 (56,1%)	20.423	84.111 (x4.12)
5	Coataxacla (Veracruz)	3.667	0.900 (24.5%)	11.181	24.117 (x2.16)
6	S. Juan Tlape (Puebla)	3.418	2.273 (66.5%)	8.821	41.733 (x4.73)
7	Ixmiquilpán (Hidalgo)	0.160	0.086 (53.8%)	0.586	1.426 (x2.43)
8	Afajayucán (Hidalgo)	0.132	0.050 (37.9%)	0.270	0.371 (x1.37)
On average:		*44.4% of the overall year exposure*		*x2.61 the mean annual DRWP*	

Tropical cyclone ***Alex*** (Atlantic Ocean)
Category 2. First impact on land: June 27, 2010
Affected zones: Campeche, Coahuila, Nuevo León, Quintana Roo and Tamaulipas

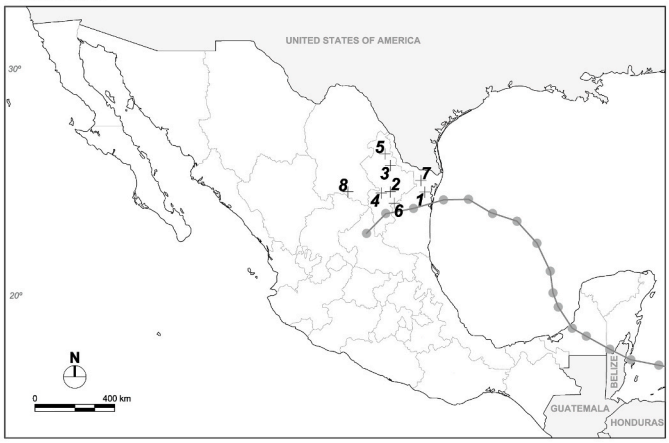

No.	Weather stations	2010 *daDRI* [m²/s]	Event contribution [m²/s]	2010 *dDRWP* [Pa]	Peak of the event [Pa]
1	S. Lorenzo (Tamaulipas)	3.583	1.625 (45.4%)	9.836	38.587 (x3.92)
2	Rancho Mª Josefina (Nuevo León)	3.767	0.490 (13.0%)	20.828	83.938 (x4.03)
3	CRFGV-UANL (Nuevo León)	2.041	0.477 (23.4%)	6.416	8.202 (x1.28)
4	Laguna de Sánchez (Nuevo León)	1.618	0.410 (25.3%)	2.760	12.105 (x4.39)
5	Anáhuac (Nuevo León)	1.528	0.639 (41.8%)	4.899	11.793 (x2.41)
6	Altavista (Nuevo León)	1.504	0.656 (43.6%)	1.570	8.042 (x5.12)
7	Galeana (Tamaulipas)	0.879	0.108 (12.3%)	7.163	20.358 (x2.84)
8	Parras el Alto (Coahuila)	0.712	0.135 (19.0%)	4.644	10.031 (x2.16)
On average:		*28.0% of the overall year exposure*		*x2.65 the mean annual DRWP*	

Tropical cyclone ***Karl*** (Atlantic Ocean)
Category 3. First impact on land: September 15, 2010
Affected zones: Campeche, Puebla, Quintana Roo and Veracruz

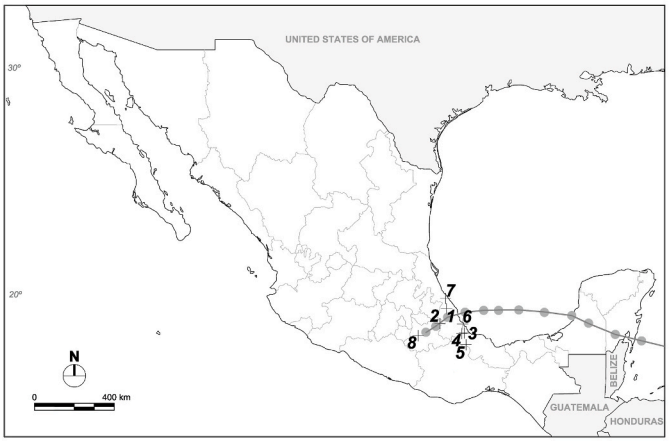

No.	Weather stations	2010 *daDRI* [m²/s]	Event contribution [m²/s]	2010 *dDRWP* [Pa]	Peak of the event [Pa]
1	INIFAP Ixatuaco (Veracruz)	12.057	10.369 (86.0%)	44.606	251.658 (x5.64)
2	Rancho Alfonso (Puebla)	9.913	8.494 (85.7%)	47.040	841.052 (x17.88)
3	Coataxacla (Veracruz)	8.726	2.320 (26.6%)	34.168	63.901 (x1.87)
4	Ignacio Palotal (Veracruz)	8.165	6.086 (74.5%)	2.684	2.851 (x1.06)
5	La Granja (Veracruz)	4.198	0.544 (13.0%)	3.007	2.870 (x0.95)
6	Úrsula Gaván (Veracruz)	2.481	0.424 (17.1%)	11.523	138.077 (x11.98)
7	Gutiérrez Zamora (Veracruz)	2.090	0.761 (36.4%)	1.348	6.260 (x4.64)
8	S. Javier (Puebla)	1.573	1.116 (70.9%)	3.248	2.076 (x0.64)
On average:		*50.0% of the overall year exposure*		*x5.58 the mean annual DRWP*	

Tropical cyclone ***Odile*** (Pacific Ocean)
Category 3. First impact on land: September 14, 2014
Affected zones: Baja California, Baja California Sur, Colima, Guerrero, Jalisco, Michoacán, Nayarit, Oaxaca, Sinaloa and Sonora

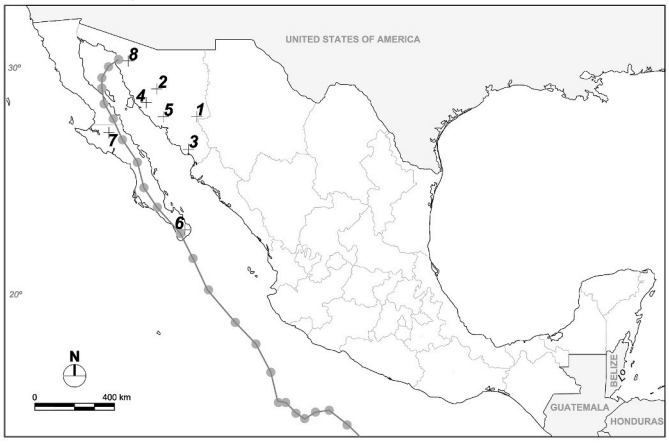

No.	Weather stations	2014 *daDRI* [m²/s]	Event contribution [m²/s]	2014 *dDRWP* [Pa]	Peak of the event [Pa]
1	Yécora (Sonora)	1.578	0.207 (13.1%)	1.726	6.006 (x3.48)
2	Selva (Sonora)	0.953	0.372 (39.0%)	3.238	11.252 (x3.47)
3	La Regla (Sonora)	0.781	0.206 (26.4%)	2.835	3.512 (x1.24)
4	Sta. Elena (Sonora)	0.695	0.266 (38.3%)	7.048	28.589 (x4.06)
5	La Campana (Sonora)	0.685	0.145 (21.2%)	3.461	11.368 (x3.28)
6	Miraflores (B. California Sur)	0.506	0.104 (20.6%)	0.464	1.325 (x2.86)
7	Rancho La Joya (B. California Sur)	0.116	0.028 (24.1%)	6.230	32.291 (x5.18)
8	El Pedernal (Sonora)	0.074	0.008 (10.8%)	0.594	1.252 (x2.11)
On average:		*24.2% of the overall year exposure*		*x3.21 the mean annual DRWP*	

Fig. 6. Temporary contribution of different tropical cyclones to the *daDRI* and *dDRWP* annual values. *Each map shows the path of the cyclone and the location of the analysed stations.*

Saffir-Simpson scale [41,42]:

• Tropical cyclone 'Dean'

Formed on 12th August 2007 approximately 840 km west of the Cape Verde Islands, this cyclone travelled a total of 7,560 km during 228 h since 1988, it was the second hurricane of category 5 to impact Mexico, surpassing the destructive hurricanes 'Kenna' (2002) and 'Wilma' (2005) in intensity. It reached the highest category on 20th of August, with sustained winds of 72.2 m/s and wind gusts of up to 87.5 m/s. After crossing the Yucatán Peninsula (leaving moderate rainfall with maximums of 81 l/m^2·day in Quintana Roo), the next day, its second impact on land occurred north of the state of Veracruz, with sustained winds of up to 43.1 m/s, wind gusts of 54.2 m/s, and intense rainfall of up to 212 l/m^2·day.

• Tropical cyclone 'Alex'

It originated on 12th June 2010 from a tropical wave in West Africa and moved slowly through the Intertropical Convergence Zone until reaching tropical storm intensity on the 26th of June, shortly before impacting Belize. After strengthening in the Gulf of Mexico, it reached category 2, a total diameter of approximately 900 km, maximum sustained winds of 45.8 m/s, and gusts of 56.9 m/s. It impacted again in Tamaulipas on the 30th June causing rainfall records of up to 446.5 l/m^2·day in the state of Nuevo León.

• Tropical cyclone 'Karl'

During 84 h, this cyclone travelled approximately 1,470 km from its origin in the Northwest Caribbean Sea, reaching category 3 on 17th September 2010 (after crossing the Yucatán Peninsula as a tropical storm). Its second impact on the north coast of the state of Veracruz caused maximum sustained winds of 54.2 m/s, gusts of 66.7 m/s, and rainfall records of up to 355 l/m^2·day.

• Tropical cyclone 'Odile'

It formed on 10th September 2014 at 385 km southwest of the city of Acapulco and had a total duration of 180 h and a global displacement of 2,560 km. It impacted as a category 3 hurricane in the south of the Baja California Peninsula on the 14th September, causing maximum sustained winds of 56.9 m/s, wind gusts of 69.4 m/s, and rainfall of up to 173 l/m^2·day in the nearby state of Sonora.

Eight meteorological stations located close to the path of each tropical cyclone were selected, attending to the criteria of continuity of the climatic data available during the event, distance variety from the eye of the hurricane, and annual exposure variety. On each of these stations (Fig. 6), the WDR and DRWP annual values of the occurrence year were compared with the temporary exposures associated with the tropical cyclone. For the WDR, all the *daDRI* values within the wetting interval associated with the tropical cyclone were added. For this purpose, a definition equivalent to that established by the standard ISO 15927–3 was adopted: each wetting interval ends with the arrival of 96 h without WDR [30]. For the DRWP, the maximum *dDRWP* value recorded within the wetting interval was identified and found to match one of the days of passage of the tropical cyclone.

Although there is wide variability in these temporary exposures depending on the residual intensity of the cyclone, the location of each station, and the duration of the wetting interval, some general patterns can be identified. These extreme atmospheric events can cause WDR values that are equivalent to those occurring in the rest of the year. The highest contributions to the annual WDR were identified during the cyclone 'Karl' with an average value of 50.0% (ranging from 86.0% in Ixatuaco to 13.0% in La Granja station). In turn, the tropical cyclone 'Odile' presented the lowest contributions to the annual WDR (24.2% on average), ranging from 10.8% in El Pedernal station to 39.0% in Selva (Sonora).

The contribution of these extreme climatic events to the annual WDR is minor in locations with lower annual values and a dry climate (see the cyclones 'Alex' and 'Odile'). This pattern, apparently counterintuitive, can be explained by the intensity loss of the cyclones with increasing latitude when moving towards the inlands of the country (i.e. the areas with lower annual WDR values). Thus, temporary exposures increase as the tropical cyclone impacts further south, both in magnitude and in its relative contribution to the annual WDR value of the locations.

In turn, the peak DRWP values during these events can exceed several times the annual mean values in most of the stations. The highest temporary DRWP values occurred during the cyclone 'Karl' (daily peaks, on average, five times greater than the mean annual *dDRWP*). Some stations, such as Rancho Alfonso (Puebla), exceeded their annual mean value by more than 15 times during the passage of the cyclone (Fig. 6). However, at other stations, the peak *dDRWP* value was even lower than the annual average (La Granja and S. Javier stations). This can be explained by the complex interaction between the direction of the prevailing winds during the cyclone and the mountainous topography around both stations. On average, temporary DRWP values about 3.5 times higher than the mean annual values are identified (x3.67, specifically), although much higher thresholds can also be observed given the variability of distances to the cyclone path, category of intensity, altitude and surroundings of the weather station, etc.

Although the passage of tropical cyclones lasts only for 2 or 3 days, the duration of the wetting intervals can be prolonged for several weeks or months depending on the climatic context of each site. The longest wetting interval was identified at the Ignacio Palotal station (cyclone 'Karl', 134 days without 96 consecutive hours lacking WDR). The shortest one corresponds to the stations of S. Juan Taple (cyclone 'Dean') and El Pedernal (cyclone 'Odile'), with a wetting interval of just 2 days. In general, the shortest wetting intervals were identified during the cyclones with higher latitude in their path (13 days on average in the stations analysed during the cyclone 'Alex' and 19 days for the cyclone 'Odile') as a result of the arid climate of these regions. Conversely, wetting intervals of up to 48 days on average were reached in the stations analysed for the cyclone 'Karl' and 47 days during the cyclone 'Dean' (both with paths in lower latitudes).

This preliminary analysis of temporary exposures complements the previous characterisation of mean annual exposures offering for the first time an exhaustive characterisation of the risk of rainwater penetration on façades throughout Mexico. This opens the door to improving the building codes and façade design standards of the country and to establishing design requirements adjusted to the specific conditions of each region.

Although this characterisation provides immediate advantages for practitioners, researchers, and Mexican institutions, it also opens up new lines of work to improve its accuracy, such as:

- Including new scalar results from other Mexican weather stations (in this research, only those with wind direction records have been considered, a limitation that now dissipates owing to the identified relationships showed in Fig. 4).
- More exhaustively characterising the states of Nayarit, Jalisco, Michoacán, and Guerrero, poorly represented in the previously accessed data.
- Using specific correlations for each state instead of the general formulae shown in Fig. 4. Specific equations by state can be identified from the scalar-directional results that are tabulated in the supplementary material.
- Exhaustively analysing temporary exposures by considering a greater number of extreme climatic events or systematically characterising the WDR and DRWP values associated with all the wetting intervals (including those not linked to tropical cyclones). In this sense, the temporary WDR and DRWP exposures shown in Fig. 6 could also be related to the average annual exposures identified at each location (see supplementary material), in order to propose general coefficients to estimate temporary exposures from the mean annual ones. However, authors discourage this procedure, since the analysis performed is still too limited to establish reliable designs (only preliminary patterns have been identified regarding these temporary exposures).

5. Conclusion

This work has developed a comprehensive characterisation of the wind-driven rain and driving rain wind pressure that determines the risk of rainwater penetration into Mexican façades. By producing exhaustive isopleth maps that represent the scalar value of the mean annual exposures, the plains of the state of Veracruz, the foothills of the Sierra Madre Sur near the Isthmus of Tehuantepec, and the easternmost part of the Trans-Mexican Volcanic Belt were identified as the most exposed areas of the country. However, most Mexican territory presents low annual exposure values. The risk of rainwater penetration in most of the locations comes mainly from the rainwater supply (given the low DRWP values), which can especially affect building façades with significant cracks, pores, and openings, what is usually present in poorly preserved buildings.

Regressions that allow the functional estimation of maximum directional exposure anywhere in the country were obtained (on the basis of these scalar maps and in locations lacking wind direction records). High temporary values of WDR and DRWP were identified in the southern regions of Mexico due to the longer duration of the wetting intervals on the façades and the higher impact seasonal tropical cyclones. Considering some extreme climatic events, temporary WDR values that can concentrate up to half of the annual average exposure as well as peak DRWP values at least 3.5 times higher than the annual values were identified.

The present results should improve the façade designs in Mexico by allowing the adjustment of watertightness requirements to the actual exposure at each site and thus minimising the grave problems currently associated with rainwater penetration into building envelopes.

CRediT authorship contribution statement

José M. Pérez-Bella: Writing – review & editing, Writing – original draft, Validation, Supervision, Methodology, Data curation, Conceptualization. **Javier Domínguez-Hernández:** Writing – review & editing, Validation, Supervision, Resources, Formal analysis. **Juan J. del Coz-Díaz:** Supervision, Project administration, Funding acquisition. **Juan E. Martínez-Martínez:** Methodology, Investigation, Data curation.

Declaration of competing interest

The authors declare that they have no known competing financial interests or personal relationships that could have appeared to influence the work reported in this paper.

Acknowledgments

These results were obtained from data provided by the National Laboratory of Modeling and Remote Sensors – LNMYSR (Government of Mexico) and by the Network of automatic weather stations in Sonora (Mexican Committee of Plant Health - CESAVE). The authors of this paper acknowledge the financial support provided by the Ministry of Science, Innovation and Universities through the National Project PGC2018-098459-B-I00. We also recognise engineers Guillermo M. Farina García, Pablo Guallar García, Jesús M. Monasterio Barricarte, Sergio Pérez Acín, and Anibal Santiago Ciprián for their help in the data collection and processing.

Appendix A. Supplementary data

Supplementary data to this article can be found online at https://doi.org/10.1016/j.buildenv.2022.108837.

References

[1] Mexican National Institute of Statistic and Geography (Inegi), Climatological and topographic maps. http://en.www.inegi.org.mx/datos/, 2021. (Accessed 23 March 2021).
[2] National center for disaster prevention (CENAPRED), Government of Mexico, Atlas climatológico de ciclones tropicales en México (Climatological atlas of tropical cyclones in Mexico, in Spanish). https://agua.org.mx/biblioteca/atlas-climatologico-de-ciclones-tropicales-en-mexico/, 2002. (Accessed 23 March 2021).
[3] Government of Mexico, Código de edificación de la vivienda 2017 (Dwelling Building Code 2017, in Spanish), Section 3001.2. https://www.gob.mx/cms/uploads/attachment/file/320345/CEV_2017_Final_.pdf (accessed 23 March 2021).
[4] D. Bastien, M. Winther-Gaasvig, Influence of driving rain and vapour diffusion on the hygrothermal performance of a hygroscopic and permeable building envelope, Energy 164 (2018) 288–297, https://doi.org/10.1016/j.energy.2018.07.195.
[5] J.M. Pérez, J. Domínguez, E. Cano, M. Alonso, J.J. del Coz, Detailed territorial estimation of design thermal conductivity for façade materials in North-Eastern Spain, Energy Build. 102 (2015) 266–276, https://doi.org/10.1016/j.enbuild.2015.05.025.
[6] A. Erkal, D. D'Ayala, L. Sequeira, Assessment of wind-driven rain impact, related surface erosion and surface strength reduction of historic building materials, Build. Environ. 57 (2012) 336–348, https://doi.org/10.1016/j.buildenv.2012.05.004.
[7] W. Tang, C.I. Davidson, S. Finger, K. Vance, Erosion of limestone building surfaces caused by wind-driven rain. 1. Field measurements, Atmos. Environ. 38 (33) (2004) 5589–5599, https://doi.org/10.1016/j.atmosenv.2004.06.030.
[8] WHO, Environmental Burden of Disease Associated with Inadequate Housing. Methods for Quantifying Health Impacts of Selected Housing Risks in the WHO European Region, World Health Organization, Copenhagen, 2011.
[9] R. Sauni, J.H. Verbeek, J. Uitti, M. Jauhiainen, K. Kreiss, T. Sigsgaard, Remediating buildings damaged by dampness and mould for preventing or reducing respiratory tract symptoms, infections and asthma, Cochrane Database Syst. Rev. (2) (2015) CD007897, https://doi.org/10.1002/14651858.CD007897.pub3.
[10] S.M. Cornick, M.A. Lacasse, A review of climate loads relevant to assessing the watertightness performance of walls, windows, and wall-window interfaces, J. ASTM Int. (JAI) 2 (10) (2005) 1–16, https://doi.org/10.1520/JAI12505.
[11] B. Blocken, J. Derome, J. Carmeliet, Rainwater runoff from building façades: a review, Build. Environ. 60 (2013) 339–361, https://doi.org/10.1016/j.buildenv.2012.10.008.
[12] CEN, EN 12865, Hygrothermal Performance of Building Components and Building Elements. Determination of the Resistance of External Wall Systems to Driving Rain under Pulsating Air Pressure, European Committee for Standardization, Brussels, 2001.
[13] R.E. Welsh, W.R. Skinner, R.J. Morris, A Climatology of Driving Rain Pressure for Canada (Climate and Atmospheric Research Directorate Draft Report), Environment Canada, Atmospheric Environment Service, Gatineau, 1989.
[14] J. Domínguez, J.M. Pérez, M. Alonso, E. Cano, J.J. del Coz, Assessment of water penetration risk in building façades throughout Brazil, Build. Res. Inf. 45 (5) (2016) 1–16, https://doi.org/10.1080/09613218.2016.1183441.
[15] J.M. Pérez, J. Domínguez, E. Cano, J.J. del Coz, A. Martín, Procedure for a detailed territorial assessment of wind-driven rain and driving-rain wind pressure and its implementation to three Spanish regions, J. Wind Eng. Ind. Aerod. 128 (2014) 76–89, https://doi.org/10.1016/j.jweia.2014.02.008.
[16] J.M. Pérez, J. Domínguez, E. Cano, J.E. Martínez, J.J. del Coz, Avoiding the need to directionally determine the exposure to rainwater penetration for façade designs, Build. Environ. 176 (2020) 106850, https://doi.org/10.1016/j.buildenv.2020.106850.
[17] A. Monterroso, C. Conde, Exposure to climate and climate change in Mexico, Geomatics, Nat. Hazards Risk 6 (4) (2015) 272–288, https://doi.org/10.1080/19475705.2013.847867.
[18] B. Blocken, J. Carmeliet, A review of wind-driven rain research in building science, J. Wind Eng. Ind. Aerod. 92 (13) (2004) 1079–1130, https://doi.org/10.1016/j.jweia.2004.06.003.
[19] B. Blocken, J. Carmeliet, Overview of three state-of-the-art wind-driven rain assessment models and comparison based on model theory, Build. Environ. 45 (3) (2010) 691–703, https://doi.org/10.1016/j.buildenv.2009.08.007.
[20] H. Ge, V. Chiu, T. Stathopoulos, Effect of overhang on wind-driven rain wetting of façades on a mid-rise building: field measurements, Build. Environ. 188 (2017) 234–250, https://doi.org/10.1016/j.buildenv.2017.03.034.
[21] A. Kubilay, D. Derome, B. Blocken, J. Carmeliet, Wind-driven rain on two parallel wide buildings: field measurements and CFD simulations, J. Wind Eng. Ind. Aerod. 146 (2015) 11–28, https://doi.org/10.1016/j.jweia.2015.07.006.
[22] N. Sahal, Proposed approach for defining climate regions for Turkey based on annual driving rain index and heating degree-days for building envelope design, Build. Environ. 41 (2006) 520–526, https://doi.org/10.1016/j.buildenv.2005.07.004.
[23] C. Giarma, D. Aravantinos, On building components' exposure to driving rain in Greece, J. Wind Eng. Ind. Aerod. 125 (2014) 133–145, https://doi.org/10.1016/j.jweia.2013.11.014.
[24] T. Qian, H. Zhang, Assessment of long-term and extreme exposure to wind-driven rain for buildings in various regions of China, Build. Environ. 189 (2021) 107524, https://doi.org/10.1016/j.buildenv.2020.107524.
[25] S.A. Orr, H. Viles, Characterisation of building exposure to wind-driven rain in the UK and evaluation of current standards, J. Wind Eng. Ind. Aerod. 180 (2018) 88–97, https://doi.org/10.1016/j.jweia.2018.07.013.

[26] J.M. Pérez, J. Domínguez, E. Cano, J.J. del Coz, M. Alonso, Global analysis of building façade exposure to water penetration in Chile, Build. Environ. 70 (2013) 284–297, https://doi.org/10.1016/j.buildenv.2013.09.001.
[27] P. Narula, K. Sarkar, S. Azad, Indexing of driving rain exposure in India based on daily gridded data, J. Wind Eng. Ind. Aerod. 175 (2018) 244–255, https://doi.org/10.1016/j.jweia.2018.02.003.
[28] R.E. Lacy, H.C. Shellard, An index of driving rain, Meteorol. Mag. 91 (1080) (1962) 177–184.
[29] J.F. Straube, E.F.P. Burnett, Simplified prediction of driving rain deposition, in: Proceedings of International Building Physics Conference, Eindhoven, 2000, pp. 375–382.
[30] CEN, EN ISO 15927-3, Hygrothermal Performance of Buildings - Calculation and Presentation of Climatic Data Part 3: Calculation of a Driving Rain Index for Vertical Surfaces from Hourly Wind and Rain Data, European Committee for Standardization, Brussels, 2009.
[31] J.M. Pérez, J. Domínguez, E. Cano, J.J. del Coz, F.P. Álvarez, On the significance of the climate-dataset time resolution in characterising wind-driven rain and simultaneous wind pressure. Part II: directional analysis, Stoch. Environ. Res. Risk Assess. 32 (2018) 1799–1815, https://doi.org/10.1007/s00477-017-1480-2.
[32] M. Arce, S. García, N. Van den Bossche, Pressure-equalised façade systems: evaluation of current watertightness test standards used to assess the performance of enclosure components, J. Build. Phys. 43 (5) (2020) 369–397, https://doi.org/10.1177/1744259119880284.
[33] N. Van der Bossche, M.A. Lacasse, T. Moore, A. Janssens, Water infiltration through openings in a vertical plane under static boundary conditions, in: Proceedings 5th International Building Physics Conference, International Association of Building Physics, Kyoto, 2012, pp. 457–463.
[34] B.A. Baskaran, W.C. Brown, Dynamic evaluation of the building envelope for wind and wind-driven rain performance, J. Build. Phys. 18 (3) (1995) 261–275, https://doi.org/10.1177/109719639501800306.
[35] National Laboratory of Modeling and Remote Sensors (INMYSR), Government of Mexico, daily data. https://clima.inifap.gob.mx/lnmysr/Principal/Index, 2020. (Accessed 23 October 2020).
[36] Network of automatic weather stations in Sonora (Mexican Committee of Plant Health – CESAVE), Weather stations. http://www.siafeson.com/remas2/index.php/estacionglobal/estaciones, 2021. (Accessed 23 March 2021).
[37] WMO, Guide to Meteorological Instruments and Methods of Observation (WMO-No 8), World Meteorological Organization, Geneva, 2008.
[38] H.E. Beck, N.E. Zimmermann, T.R. McVicar, N. Vergopolan, A. Berg, E.F. Wood, Present and future Köppen-Geiger climate classification maps at 1-km resolution, Sci. Data 5 (2018) 180214, https://doi.org/10.1038/sdata.2018.214.
[39] J. Larson, Y. Zhou, R.W. Higgins, Characteristics of landfalling tropical cyclones in the United States and Mexico: climatology and interannual variability, J. Clim. 18 (2005) 1247–1262, https://doi.org/10.1175/JCLI3317.1.
[40] T. Baheru, A.G. Chowdhury, G. Bitsuamlak, F.J. Masters, A. Tokay, Simulation of wind-driven rain associated with tropical storms and hurricanes using the 12-fan Wall of Wind, Build. Environ. 76 (2014) 18–29, https://doi.org/10.1016/j.buildenv.2014.03.002.
[41] J. Camelo, T. Mayo, The lasting impacts of the Saffir-Simpson Hurricane Wind Scale on storm surge risk communication: the need for multidisciplinary research in addressing a multidisciplinary challenge, Weather Clim. Extremes 33 (2021) 100335, https://doi.org/10.1016/j.wace.2021.100335.
[42] National Water Commission (CONAGUA), Government of Mexico, Consultation of history and summaries of tropical cyclones. https://smn.conagua.gob.mx/es/ciclones-tropicales/informacion-historica, 2021. (Accessed 23 March 2021).
[43] R. Pacheco, J. Ordóñez, G. Martínez, Energy efficient design of building: a review, Renew. Sustain. Energy Rev. 16 (2012) 3559–3573, https://doi.org/10.1016/j.rser.2012.03.045.
[44] J.L. Devore, Probability & Statistics for Engineering and the Sciences, eighth ed., Cengage Learning, Boston, 2010.
[45] J.M. Pérez, J. Domínguez, B. Rodríguez, J.J. del Coz, E. Cano, Combined use of wind-driven rain and wind pressure to define water penetration risk into building façades: the Spanish case, Build. Environ. 64 (2013) 46–56, https://doi.org/10.1016/j.buildenv.2013.03.004.
[46] S.A. Orr, M. Cassar, Exposure indices of extreme wind-driven rain events for built heritage, Atmosphere 11 (2) (2020) 163, https://doi.org/10.3390/atmos11020163.
[47] T. Baheru, A.G. Chowdhury, J.P. Pinelli, Estimation of wind-driven rain intrusion through building envelope defects and breaches during tropical cyclones, Nat. Hazards Rev. 16 (2015) 2, https://doi.org/10.1061/(ASCE)NH.1527-6996.0000158.
[48] X. Wang, Q. Li, J. Li, Field measurements and numerical simulations of wind-driven rain on a low-rise building during typhoons, J. Wind Eng. Ind. Aerod. 204 (2020) 104274, https://doi.org/10.1016/j.jweia.2020.104274.